ResearchGate

See discussions, stats, and author profiles for this publication at: https://www.researchgate.net/publication/44887071

Probing Slow Protein Dynamics by Adiabatic R−1 rho and R−2 rho NMR Experiments

ARTICLE *in* JOURNAL OF THE AMERICAN CHEMICAL SOCIETY · JULY 2010

Impact Factor: 12.11 · DOI: 10.1021/ja1038787 · Source: PubMed

CITATIONS
18

READS
24

5 AUTHORS, INCLUDING:

Silvia Mangia
Center for Magnetic Resonance Research Min…
61 PUBLICATIONS **912** CITATIONS
SEE PROFILE

Gianluigi Veglia
University of Minnesota Twin Cities
173 PUBLICATIONS **3,830** CITATIONS
SEE PROFILE

Michael Garwood
University of Minnesota Twin Cities
280 PUBLICATIONS **8,833** CITATIONS
SEE PROFILE

Shalom Michaeli
University of Minnesota Twin Cities
49 PUBLICATIONS **880** CITATIONS
SEE PROFILE

Available from: Michael Garwood
Retrieved on: 24 January 2016

NIH Public Access
Author Manuscript
J Am Chem Soc. Author manuscript; available in PMC 2011 July 28.

Published in final edited form as:
J Am Chem Soc. 2010 July 28; 132(29): 9979–9981. doi:10.1021/ja1038787.

Probing Slow Protein Dynamics by Adiabatic $R_{1\rho}$ and $R_{2\rho}$ NMR Experiments

Silvia Mangia[1,*,‡], **Nathaniel J. Traaseth**[2,‡], **Gianluigi Veglia**[2,3,*], **Michael Garwood**[1], and **Shalom Michaeli**[1]

[1] Center for Magnetic Resonance Research, Department of Radiology, University of Minnesota, Minneapolis, Minnesota, USA

[2] Department of Molecular Biology and Biophysics, University of Minnesota, Minneapolis, Minnesota, USA

[3] Department of Chemistry and Biochemistry, University of Minnesota, Minneapolis, Minnesota, USA

Abstract

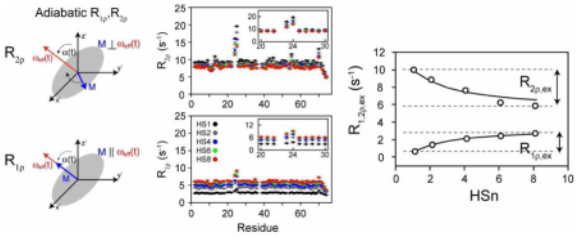

Slow μsec/msec dynamics involved in protein folding, binding, catalysis and allostery are currently detected using NMR dispersion experiments such as CPMG (Carr-Purcell-Meiboom-Gill) or spin-lock $R_{1\rho}$. In these methods, protein dynamics are obtained by analyzing relaxation dispersion curves obtained from either changing the time-spacing between 180° pulses or by changing the effective spin-locking field strength. In this Communication, we introduce a new method to induce a dispersion of relaxation rates. Our approach relies on altering the shape of the adiabatic full passage pulse, and is conceptually different from existing approaches. By changing the nature of the adiabatic radiofrequency irradiation, we are able to obtain rotating frame R_1 and R_2 ($R_{1\rho}$ and $R_{2\rho}$) dispersion curves that are sensitive to slow μsec/msec protein dynamics (demonstrated with ubiquitin). The strengths of this method are to (a) extend the dynamic range of the relaxation dispersion analysis, (b) avoid the need for multiple magnetic field strengths to extract dynamic parameters, (c) measure accurate relaxation rates that are independent of frequency offset, and (d) reduce the stress to NMR hardware (e.g., cryoprobes).

Protein dynamics is central to function. Specifically, conformational dynamics in the μsec-msec timescale is synchronous with phenomena such as allostery, folding, molecular recognition, catalysis and inhibition.[1–11]

mangia@cmrr.umn.edu, vegli001@umn.edu.
‡The authors contributed equally to this work

Supporting Information Available: The pulse shape profiles (frequency and amplitude modulation) as a function of the AFP pulse duration are given for the five HSn pulses that were employed in this study. The adiabatic pulses and pulse sequence code (for Varian spectrometers) are available for download at our website: www.chem.umn.edu/groups/veglia.

NIH-PA Author Manuscript
NIH-PA Author Manuscript
NIH-PA Author Manuscript

NIH-PA Author Manuscript

NIH-PA Author Manuscript

NIH-PA Author Manuscript

NMR rotating frame ($R_{1\rho}$) and Carr-Purcell-Meiboom-Gill (CPMG, R_2) relaxation dispersion methods have been widely used to probe slow dynamics and discriminate ground and excited states in small and large proteins.[12, 13] While these approaches have been critical in characterizing enthalpy and entropy in biomolecules, the methods are limited by (a) the small dynamic range of the relaxation dispersion phenomena, (b) difficulty in setting up the pulse sequences, (c) the low tolerance of cryogenic probes for continuous radiofrequency (RF) irradiation, and (d) the cost of performing relaxation measurements at multiple magnetic fields in order to extract reliable dynamic parameters. To expand the dynamic range of relaxation dispersions, sample conditions are often changed (pH, temperature, viscosity, *etc.*). While there have been some technical improvements to the CPMG method,[14, 15] there have been no good remedies for the other drawbacks.

In this Communication, we present a conceptually different method for characterizing slow μsec/msec protein motions. Our approach consists of using adiabatic full passage (AFP) pulses[16] to induce a dispersion of relaxation rates, which expands the dynamic range and substantially increases the ease for measuring relaxation dispersion experiments. Unlike the CPMG R_2 or spin-lock $R_{1\rho}$ dispersion experiments (reviewed in Ref. [17]), where relaxation dispersion is obtained by changing the duration between 180° pulses or the spinlocking field strength, we altered the shape of the adiabatic RF irradiation to obtain $R_{1\rho}$ and $R_{2\rho}$ dispersion curves. Contrast in relaxation rates can be generated by use of adiabatic RF pulses,[16] which enables the coverage of large bandwidths with relatively low power. While adiabatic pulses have been incorporated in many biomolecular NMR experiments,[18] the concept of using adiabatic RF pulses to induce relaxation dispersion has not been introduced.

We tested this approach with ubiquitin, a globular protein whose dynamics has been recognized to be crucial for proteinprotein recognition.[19] Adiabatic $R_{1\rho}$ and $R_{2\rho}$ relaxation rates [20–22] were measured at 14.1 T (600 MHz ^{1}H frequency) on a sample of [U-^{15}N] labeled ubiquitin at 5 °C and 25 °C. A standard 2D HSQC-type pulse sequence (Figure 1)[23] was modified by inserting ^{15}N pulse trains of 4, 8, 12, 16, 20, 24 and 28 AFP pulses. The relaxation experiments were conducted such that the magnetization rotated in a perpendicular ($R_{2\rho}$) direction around the effective field or was aligned with it ($R_{1\rho}$). Adiabatic hyperbolic secant (HS) pulses were designed with different “stretching” factors (HSn: n = 1, 2, 4, 6 and 8).[24] The applied RF amplitude ($\omega_1(t)$) and frequency sweep ($\omega_{RF}(t) - \omega_c$) of the HSn AFP pulses are:

$$\omega_1(t)=\omega_1^{max}\,\mathrm{sech}[\beta(2t/T_p-1)^n] \quad (1)$$

$$\omega_{RF}(t)-\omega_c=\frac{BW}{2}\int_0^t \mathrm{sech}^2[\beta(2t'/T_p-1)^n]dt' \quad (2)$$

where ω_1^{max} is the maximum amplitude of the pulse, β is a truncation factor (sech(β)=0.01), T_p is the length of the AFP pulse, ω_c is the carrier frequency, BW is the bandwidth of the pulse, and t and t′ represent time. Note that ω_1, ω_1^{max}, ω_{RF}, ω_c and BW are expressed in units of rad/s. Each AFP pulse was 4-msec and implemented in groups of four (phase-cycled using MLEV-4[25]), leading to total relaxation delays of 16, 32, 48, 64, 80, 96 and 112 msec (no 112 msec for $R_{2\rho}$). The maximum amplitude of the AFP pulse was $\omega_1^{max}/(2\pi)$ = 3.5 kHz, and the bandwidth, BW/(2π), was 10 kHz. This choice of parameters guaranteed full adiabatic inversion of all residues within a range of ~3 kHz for every HSn pulse. Relaxation rates were obtained in a residue dependent manner by fitting a mono-exponential decay

NIH-PA Author Manuscript

NIH-PA Author Manuscript

NIH-PA Author Manuscript

function to the signal intensities *versus* AFP-train duration. No proton decoupling scheme was used, since net evolution due to heteronuclear scalar coupling was refocused by the ^{15}N AFP pulses in the $R_{1\rho}$ and $R_{2\rho}$ experiments.[26]

Several relaxation studies have been conducted on ubiquitin, which has a compact fold with nearly all of the residues displaying similar relaxation rates. The relaxation rates measured with our methods (Figure 2) are in agreement with previous data,[27] showing essentially constant $R_{1\rho}$ and $R_{2\rho}$ rates under each of the HSn pulses. Note that adiabatic pulses cover the entire bandwidth for the ^{15}N chemical shifts. This avoids the cumbersome back-calculation of the "nominal" effective frequency and tilt angle for each residue of interest, a procedure that requires extremely accurate power calibration when using the spin-lock $R_{1\rho}$ dispersion approach.

The utilization of different modulation functions induced a dispersion of relaxation rates for all residues, with the smallest adiabatic $R_{1\rho}$ given by HS1 pulses, followed by HS2, HS4, HS6, and HS8. The opposite trend was seen for $R_{2\rho}$. Notably, residues undergoing conformational exchange (e.g., Asn25) exhibited faster adiabatic $R_{1\rho}$ and $R_{2\rho}$ and larger dispersions (i.e., the difference in relaxation rates between HS1 and HS8) as compared to residues with no conformational exchange (e.g., Lys48). Residues not undergoing exchange displayed larger $R_{1\rho}$ dispersion as compared to $R_{2\rho}$, while the opposite trend is detected for residues with a contribution from chemical exchange. The dispersion rates become considerably smaller upon increasing the temperature (Figure 2), implying that adiabatic $R_{1\rho}$ and $R_{2\rho}$ are mainly sensitive to slow exchange dynamics. Notably, no dispersion of relaxation rates (above 1 Hz) was observed for any residue at 5 °C when measured using the classical CPMG relaxation dispersion method (Figure 3). A small relaxation dispersion was observed in Asn25 using the off-resonance $R_{1\rho}$ experiment previously used to measure μsec-msec motions in ubiquitin (see Figure 3A).[27]

Although the complete description of the relaxation during adiabatic pulses would require the evaluation of chemical shift anisotropy, cross-correlated relaxation and interference effects, we assumed that relaxation phenomena not related to chemical exchange are approximately similar across the protein sequence (excluding terminal residues). Under these approximations, the difference of rates between the two kinds of residues represents purely the exchange contribution [e.g., for each HSn pulse: $R_{1,2,\rho,ex}=R_{1,2\rho}(\text{Asn25})-R_{1,2\rho}(\text{Lys48})$]. We analyzed the exchange-induced relaxations during the AFP pulses using the classical formalism developed for the fast exchange regime ($1/\tau_{ex} > \Delta\omega$).[20, 28, 29] According to this treatment, the $R_{1\rho}$ and $R_{2\rho}$ result from an average of instantaneous time-dependent contributions, arising from the inherent time evolution of the effective frequency (ω_{eff}) and the tilt angle, α, during the pulse:

$$R_{1\rho,ex}(t)=\int_0^{T_p} p_A p_B \Delta\omega^2 \sin^2\alpha(t)\frac{\tau_{ex}}{1+(\omega_{eff}(t)\tau_{ex})^2}dt \quad (3)$$

$$R_{2\rho,ex}(t)=\int_0^{T_p} p_A p_B \Delta\omega^2 \left[\cos^2\alpha(t)\tau_{ex}+\tfrac{1}{2}\sin^2\alpha(t)\frac{\tau_{ex}}{1+(\omega_{eff}(t)\tau_{ex})^2}\right]dt \quad (4)$$

p_A and p_B are the populations of the two exchanging sites, Δω is the chemical shift difference, and τ_{ex} is the exchange correlation time. For Asn25 of ubiquitin, the exchange parameters found using Eqs 3 and 4 gave $\Delta\omega^2 p_A p_B = 29 \times 10^4$ [rad/s]^2 and $1/\tau_{ex} \sim 2.5 \times 10^4$

NIH-PA Author Manuscript

NIH-PA Author Manuscript

NIH-PA Author Manuscript

s^{-1}, which are in quantitative agreement with the corresponding values reported previously.[27]

In conclusion, adiabatic rotating frame relaxation measurements, $R_{1\rho}$ and $R_{2\rho}$, provide a solid approach for characterizing μsec-msec protein dynamics. These pulse sequences are straightforward to set-up and implement on any modern spectrometer that can perform phase and amplitude RF modulation. Unlike currently available methods, this approach gives frequency offset independent relaxation rates without the need to apply residue-specific corrections. More importantly, the use of AFP extends the dynamic range of the relaxation dispersion analysis, avoiding troublesome variations of sample conditions and/or use of multiple magnetic field strengths to extract dynamic parameters. The relatively low power utilized for these pulses avoids excess stress to the hardware (probes), and at the same time substantially reduces sample heating. This approach can be applied to a wide range of relaxation measurements from small to large soluble proteins as well as membrane proteins reconstituted in detergent micelles,[30] taking advantages of TROSY schemes.[31] The implementation to other nuclei (^{1}H, ^{13}C, ^{2}H) will be highly beneficial in the characterization of both backbone and side chain dynamics in macromolecular complexes.

Supplementary Material

Refer to Web version on PubMed Central for supplementary material.

Acknowledgments

NIH Grants GM64742, HL80081, GM072701 (to G. Veglia); NIH P41 RR008079 (to CMRR); R01NS061866 and R21NS059813 (to S. Michaeli).

References

1. Boehr DD, McElheny D, Dyson HJ, Wright PE. Science. 2006; 313:1638–1642. [PubMed: 16973882]
2. Eisenmesser EZ, Millet O, Labeikovsky W, Korzhnev DM, Wolf-Watz M, Bosco DA, Skalicky JJ, Kay LE, Kern D. Nature. 2005; 438:117–121. [PubMed: 16267559]
3. Korzhnev DM, Kay LE. Acc Chem Res. 2008; 41:442–451. [PubMed: 18275162]
4. Frederick KK, Marlow MS, Valentine KG, Wand AJ. Nature. 2007; 448:325–329. [PubMed: 17637663]
5. Petit CM, Zhang J, Sapienza PJ, Fuentes EJ, Lee AL. Proc Natl Acad Sci U S A. 2009; 106:18249–18254. [PubMed: 19828436]
6. Beach H, Cole R, Gill ML, Loria JP. J Am Chem Soc. 2005; 127:9167–9176. [PubMed: 15969595]
7. Das R, Chowdhury S, Mazhab-Jafari MT, Sildas S, Selvaratnam R, Melacini G. J Biol Chem. 2009; 284:23682–23696. [PubMed: 19403523]
8. Ishima R, Louis JM, Torchia DA. J Mol Biol. 2001; 305:515–521. [PubMed: 11152609]
9. Namanja AT, Wang XJ, Xu B, Mercedes-Camacho AY, Wilson BD, Wilson KA, Etzkorn FA, Peng JW. J Am Chem Soc. 2010; 132:5607–5609. [PubMed: 20356313]
10. Kern D, Zuiderweg ER. Curr Opin Struct Biol. 2003; 13:748–57. [PubMed: 14675554]
11. Igumenova TI, Lee AL, Wand AJ. Biochemistry. 2005; 44:12627–12639. [PubMed: 16171378]
12. Mulder FA, Mittermaier A, Hon B, Dahlquist FW, Kay LE. Nat Struct Biol. 2001; 8:932–935. [PubMed: 11685237]
13. Palmer AG 3rd, Kroenke CD, Loria JP. Methods Enzymol. 2001; 339:204–238. [PubMed: 11462813]
14. Long D, Liu M, Yang D. J Am Chem Soc. 2008; 130:2432–2433. [PubMed: 18247615]
15. Yip GN, Zuiderweg ER. J Magn Reson. 2004; 171:25–36. [PubMed: 15504678]
16. Garwood M, DelaBarre L. J Magn Reson. 2001; 153:155–177. [PubMed: 11740891]

NIH-PA Author Manuscript

NIH-PA Author Manuscript

NIH-PA Author Manuscript

17. Loria JP, Berlow RB, Watt ED. Acc Chem Res. 2008; 41:214–221. [PubMed: 18281945]
18. Zweckstetter M, Holak TA. J Magn Reson. 1998; 133:134–147. [PubMed: 9654478]
19. Lange OF, Lakomek NA, Fares C, Schroder GF, Walter KF, Becker S, Meiler J, Grubmuller H, Griesinger C, de Groot BL. Science. 2008; 320:1471–1475. [PubMed: 18556554]
20. Michaeli S, Sorce DJ, Idiyatullin D, Ugurbil K, Garwood M. J Magn Reson. 2004; 169:293–299. [PubMed: 15261625]
21. Michaeli S, Sorce DJ, Springer CS Jr, Ugurbil K, Garwood M. J Magn Reson. 2006; 181:135–147. [PubMed: 16675277]
22. Mangia S, Liimatainen T, Garwood M, Michaeli S. Magn Reson Imaging. 2009; 27:1074–1087. [PubMed: 19559559]
23. Farrow NA, Muhandiram R, Singer AU, Pascal SM, Kay CM, Gish G, Shoelson SE, Pawson T, Forman-Kay JD, Kay LE. Biochemistry. 1994; 33:5984–6003. [PubMed: 7514039]
24. Tannus A, Garwood M. NMR Biomed. 1997; 10:423–434. [PubMed: 9542739]
25. Levitt M, Freeman R, Frenkel T. J Magn Reson. 1982; 47:328–30.
26. Bendall MR. J Magn Reson A. 1995; 116:46–58.
27. Massi F, Grey MJ, Palmer AG 3rd. Protein Sci. 2005; 14:735–742. [PubMed: 15722448]
28. Abergel D, Palmer AG. Conc Magn Reson. 2003; 19A:134–48.
29. Sorce DJ, Michaeli S, Garwood M. J Magn Reson. 2006; 179:136–139. [PubMed: 16298149]
30. Traaseth NJ, Veglia G. Biochim Biophys Acta. 2010; 1798:77–81. [PubMed: 19781521]
31. Pervushin K, Riek R, Wider G, Wuthrich K. Proc Natl Acad Sci U S A. 1997; 94:12366–12371. [PubMed: 9356455]

NIH-PA Author Manuscript

NIH-PA Author Manuscript

NIH-PA Author Manuscript

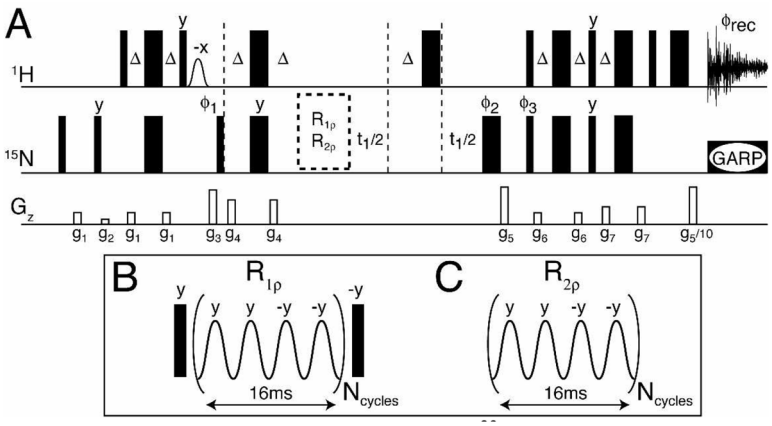

Figure 1.

HSQC-type pulse sequence[23] (A) used to measure $R_{1\rho}$ (B) and $R_{2\rho}$ (C). In the $R_{1\rho}$ experiment, ^{15}N magnetization is positioned longitudinally, and then subjected to a train of adiabatic pulses. For the $R_{2\rho}$ experiment, ^{15}N magnetization is positioned in the transverse plane, and then subjected to a train of adiabatic pulses. Note that N_{cycles} needs to be an integer value, and differs from n, the stretching factor (see Eqs. 1–2). Phases are φ_1 = x, −x, x, −x, φ_2 = x, x, y, y, φ_3 = x, φ_{rec} = x, −x, x, −x. The phases of ϕ_3 and ϕ_{rec} are both inverted (shifted by 180°) in alternate t_1 increments. Gradient magnitudes for G_1–G_7 are 1.8, 1.3, 26.6, 14.2, 42.6, 3.6 and 5.3 G/cm with lengths of 0.5, 0.5, 1, 1, 2, 0.5 and 0.5 msec, respectively. To achieve phase-sensitive t_1 detection, the phases of φ_1 and the magnitude of the second G_5 gradient are inverted (−42.6 G/cm).

NIH-PA Author Manuscript

NIH-PA Author Manuscript

NIH-PA Author Manuscript

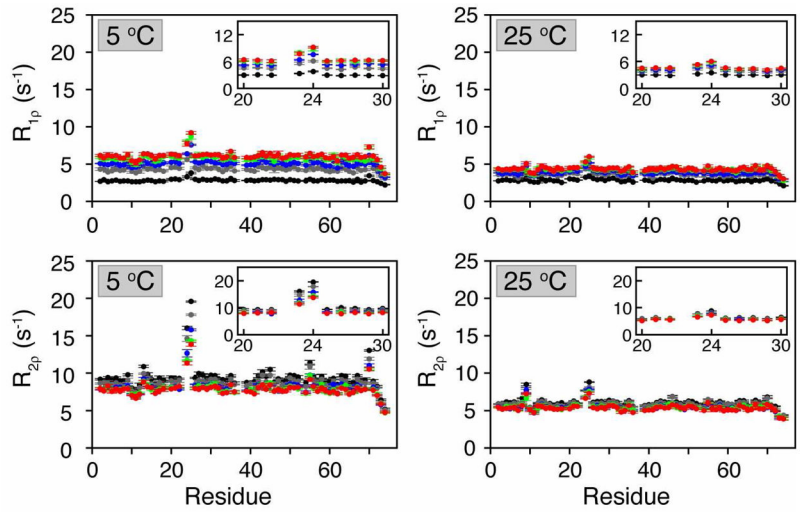

Figure 2.

$R_{1\rho}$ and $R_{2\rho}$ relaxation rates at 5 °C and 25 °C. The trends in the relaxation rates for $R_{1\rho}$ are HS1 (black) < HS2 (grey) < HS4 (blue) < HS6 (green) < HS8 (red) and for $R_{2\rho}$ are HS1 > HS2 > HS4 > HS6 > HS8, are consistent with anticipated results. [22] Residues that are known to undergo chemical exchange at 5 °C (Glu24, Asn25, Thr55 and Val70) displayed a pronounced dispersion between the HSn pulse types, which is not observed at 25 °C (i.e., exchange becomes too fast).

NIH-PA Author Manuscript
NIH-PA Author Manuscript
NIH-PA Author Manuscript

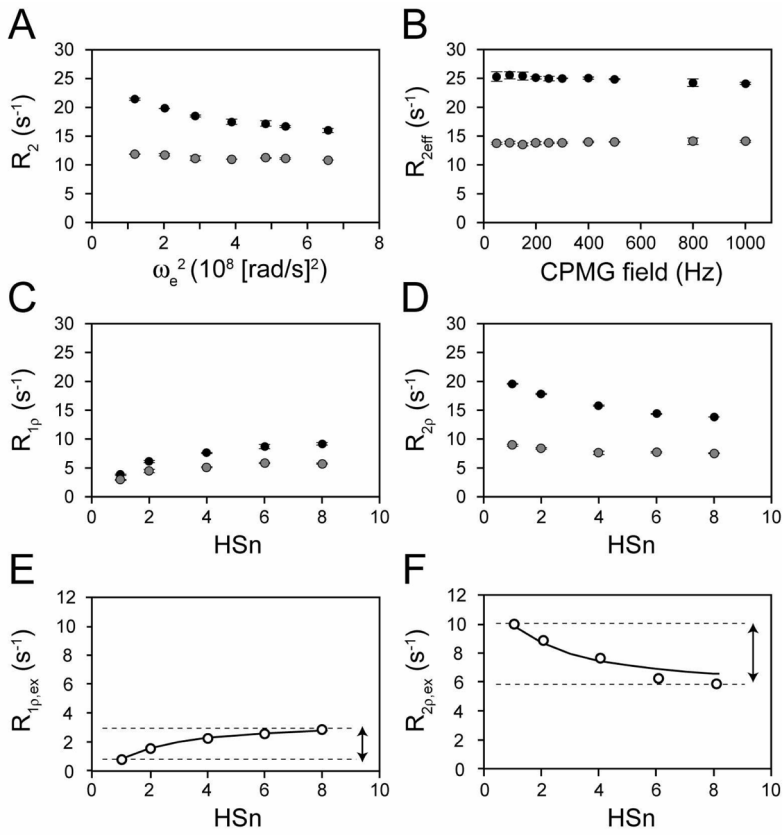

Figure 3.

Relaxation dispersion results for Asn25 (black circles) and Lys48 (grey circles) of ubiquitin collected at 5 °C. (A) $R_{1\rho}$ and (B) CPMG relaxation dispersion experiments. (C) $R_{1\rho}$ and (D) $R_{2\rho}$ relaxation rates plotted as a function of HSn adiabatic pulse. Chemical exchange contributions to $R_{1\rho}$ (E) and $R_{2\rho}$ (F) for Asn25 (open circles) obtained by subtracting the rates of Lys48 from those of Asn25. Best fits of the data to Eqs 3 and 4 give $\Delta\omega^2 p^A p^B = 29 \times 10^4$ [rad/s]^2 and $1/\tau_{ex} \sim 2.5 \times 10^4$ s^{-1}.